Shock and Vibration 19 (2012) 1115–1123
DOI 10.3233/SAV-2012-0716
IOS Press

Celtic stone dynamics revisited using dry friction and rolling resistance

J. Awrejcewicz* and G. Kudra
Department of Automation and Biomechanics, The Technical University of Lodz, Lodz, Poland

Abstract. The integral model of dry friction components is built with assumption of classical Coulomb friction law and with specially developed model of normal stress distribution coupled with rolling resistance for elliptic contact shape. In order to avoid a necessity of numerical integration over the contact area at each the numerical simulation step, few versions of approximate model are developed and then tested numerically. In the numerical experiments the simulation results of the Celtic stone with the friction forces modelled by the use of approximants of different complexity (from no coupling between friction force and torque to the second order Padé approximation) are compared to results obtained from model with friction approximated in the form of piecewise polynomial functions (based on the Taylor series with hertzian stress distribution). The coefficients of the corresponding approximate models are found by the use of optimization methods, like as in identification process using the real experiment data.

Keywords: Celtic stone, Coulomb-Contensou-Zhuravlev friction model, rolling resistance

1. Introduction

For small contact area between two bodies the sliding friction force opposes the sliding relative velocity and can be successfully modelled by the use of classical one-dimensional Coulomb friction law. But there are many cases of dynamical mechanical systems (billiard ball, Thompson top, electric polishing machine) which cannot be mathematically modelled (in order to obtain correct numerical simulation) or explained by the use of assumption of one-dimensional dry friction model.

Contensou [1] noticed that relative normal angular velocity (spin) is important for dynamics of some mechanical systems, where contact between two bodies or spin is relatively large. Basing on the Coulomb friction law he presented friction force as a function of two variables: relative sliding velocity of the centre of the non-point circular contact area between two interacting bodies and relative normal angular velocity. Then the results of Contensou were essentially developed by Zhuravlev [2] by giving exact analytical expressions for friction force and torque as well as corresponding linear Padé approximations more convenient to use in practical problems of modelling and simulation. We will refer to coupled model of friction force and torque as Coulomb-Contensou fritction model. This direction of research led then to the second-order Padé approximants [3], more accurate and suitable for qualitative analysis. A three-dimensional friction model for circular areas but with the coupling between friction and rolling resistance, where rolling resistance is a result of distortion of contact stress distribution, is developed in the work [4]. In the work [5] the modelling of celt is performed, where the spatial Coulomb-Contensou friction model with linear Padé approximations for circular contact patch is applied. However, since the friction force is the only way of dissipation in the proposed model, the time of the wobblestone motion (until rest) is unrealistically long.

In the work [6] the coupled friction model for circular contact area with central symmetry of contact stress distribution (without rolling resistance) was approximated by the use of Taylor expansion of the velocity pseudo po-

*Corresponding author: J. Awrejcewicz, Department of Automation and Biomechanics, The Technical University of Lodz, 1/15 Stefanowskiego St., 90-924 Lodz, Poland. E-mail: jan.awrejcewicz@p.lodz.pl.

ISSN 1070-9622/12/$27.50

tential and then used in the Thompson top modelling and simulation. Tangens hiperbolicus based models can also be used as good approximations of friction force and torque in the case of circular contact area with Hertz distribution with a special distortion [7].

The present work aims at the development of the coupled approximate model of dry friction force and torque as well as the rolling resistance for elliptic contact area.

2. Mathematical modeling of the Celtic stone

The wobblestone as a semi-ellipsoid rigid body with the geometry centre O and with the mass centre C (with the relative position defined by the vector $\mathbf{k}$) touching a rigid, flat and immovable horizontal surface π (parallel to the X_1X_2 plane of the global immovable coordinate system $X_1X_2X_3$) at the point A, is presented in Fig. 1.

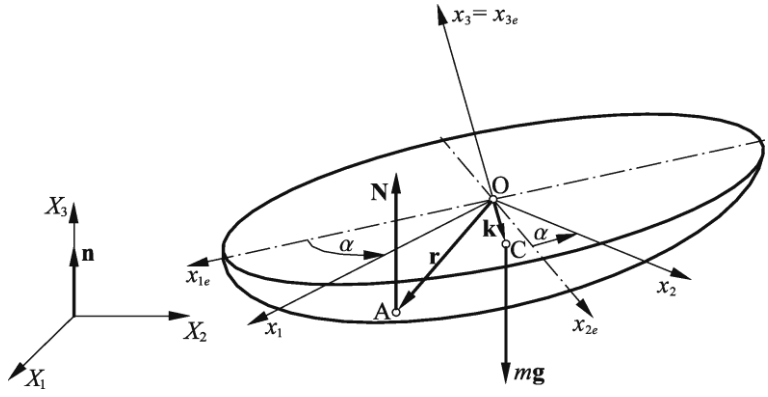

Fig. 1. The Celtic stone.

The differential equations of motion in the movable co-ordinate system $0x_1x_2x_3$ (with axes parallel to the central principal axes of inertia – we assume that the geometrical axis x_{3e} of the ellipsoid is parallel to one of them) are as follows

$$m\frac{\tilde{d}\mathbf{v}}{dt}+\boldsymbol{\omega}\times(m\mathbf{v})=-mg\mathbf{n}+\hat{N}\mathbf{n}+\hat{\mathbf{T}}_s,\quad \mathbf{B}\frac{\tilde{d}\boldsymbol{\omega}}{dt}+\boldsymbol{\omega}\times(\mathbf{B}\boldsymbol{\omega})=(\mathbf{r}-\mathbf{k})\times\left(\hat{N}\mathbf{n}+\hat{\mathbf{T}}_s\right)+\hat{\mathbf{M}}_s+\hat{\mathbf{M}}_r$$
$$\frac{\tilde{d}\mathbf{n}}{dt}+\boldsymbol{\omega}\times\mathbf{n}=0, \tag{1}$$

where m is the mass of the celt, $\mathbf{B}=\mathrm{diag}(B_1, B_2, B_3)$ is the tensor of inertia of the solid, $\mathbf{v}$ is the absolute velocity of the mass centre C, $\boldsymbol{\omega}$ is the absolute angular velocity of the body, $\hat{N}$ is the value of the normal reaction of the horizontal plane, $\mathbf{n}$ is the unit vector normal to the plane X_1X_2, $\hat{\mathbf{T}}_s$ (ignored in Fig. 1) is the sliding friction force in the point of contact A, $\hat{\mathbf{M}}_s$ and $\hat{\mathbf{M}}_r$ (ignored in Fig. 1) are the dry friction and the rolling resistance torques respectively applied to the body at point A. The notation $\tilde{d}\boldsymbol{a}/dt$ denotes the time derivative of the vector $\mathbf{a}$ in the movable body-fixed coordinate system $0x_1x_2x_3$.

Taking the ellipsoid equation and the condition of tangent contact between the ellipsoid and the horizontal plane

$$\varphi(\boldsymbol{r})=\frac{r_{x_{1e}}^2}{a_1^2}+\frac{r_{x_{2e}}^2}{a_2^2}+\frac{r_{x_{3e}}^2}{a_3^2}-1=0,\qquad \mathbf{n}=\mu\frac{d\varphi}{d\mathbf{r}}, \tag{2}$$

(where $\mu<0$ is a certain scalar multiplier and a_1, a_2 and a_3 are the semi-axes of the ellipsoid) we can find the relation between the components of the vectors $\mathbf{r}$ and $\mathbf{n}$ in the $0x_{1e}x_{2e}x_{3e}$ coordinate system. Since the $0x_1x_2x_3$ co-ordinate

system is obtained by rotation of the $0x_{1e}x_{2e}x_{3e}$ system around the x_{3e} axis by the angle α, the corresponding relation in the $0x_1x_2x_3$ co-ordinate system can be found easily.

The set of Eq. (1) consists of 9 scalar first order ordinary differential equations with 10 unknown functions of time: v_{x_i}, ω_{x_i}, n_{x_i} (i=1,2,3) and $\hat{N}$. The missing equation is the following algebraic one

$$\mathbf{v}_A \cdot \mathbf{n} = 0, \quad \text{where } \mathbf{v}_A = [\mathbf{v} + \boldsymbol{\omega} \times (\mathbf{r} - \mathbf{k})] \tag{3}$$

which follows the fact that the velocity $\boldsymbol{v}_A$ lies in the plane π. Equations (1) and (3) form now the differential-algebraic equation set. One way to solve them is to differentiate the condition Eq. (3) with respect to time and then treat it as an additional equation during solving the governing equations algebraically with respect to the corresponding unknown functions. Note that the function $\hat{N}$ appears in the models of $\hat{\mathbf{T}}_s$, $\hat{\mathbf{M}}_s$ and $\hat{\mathbf{M}}_r$ presented in the next section.

3. Friction and rolling resistance modeling

3.1. Model of normal stress distribution

We start from an assumption of certain non-dimensional normal stress $\sigma_0'(r')$ distribution over the non-dimensional circular zone $F'\left(\iint_{F'} dF' = 1\right)$ presented in Fig. 2a, where r' is one of the polar coordinates (r', φ') related to the Cartesian ones (x', y') as follows: $x' = r'\cos\varphi'$ and $y' = r'\sin\varphi'$. As a result of movement of a deformation area F' (with velocity $\boldsymbol{v}_r'$) the initial stress distribution is distorted in the following way [4]

$$\sigma'(x', y') = \sigma_0'\left(\sqrt{x'^2 + y'^2}\right)\left(1 + k_r x'\cos\gamma' + k_r y'\sin\gamma'\right) \tag{4}$$

producing a rolling resistance, where $0 \leqslant k_r \leqslant 1$ is a rolling resistance parameter.

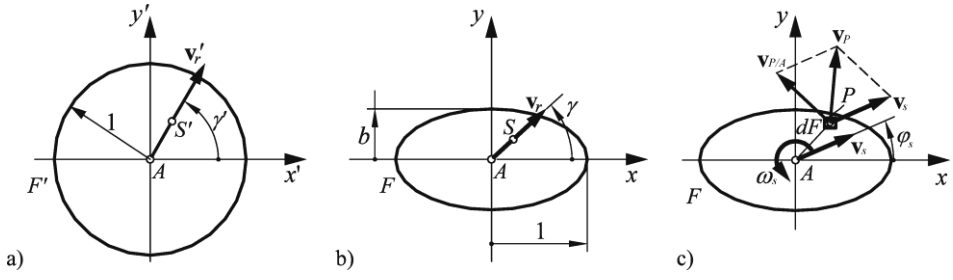

Fig. 2. Elliptic contact area between two bodies with the co-ordinate systems.

Then we try to extend the model used in the work [4] by contraction of the circular area F' along the y' axis. We obtain the non-dimensional elliptic contact zone F exhibited by Fig. 2b with Cartesian coordinates (x, y) of any point position, related to the (x', y') ones as $x = x'$ and $y = by'$. The stress distribution $\sigma(x, y) = b^{-1}\sigma'(x, y)$ over the contracted area F reads as follows

$$\sigma(x, y) = b^{-1}\sigma_0'\left(\sqrt{x^2 + b^{-2}y^2}\right)\left(1 + k_r x\cos\gamma' + k_r b^{-1} y\sin\gamma'\right). \tag{5}$$

We assume that the quantities used to describe the model of friction refer to the dimensionless length related to the real length of the major semi-axis $\hat{a}$, therefore dimensionless coordinates of any point on contact area are $x = \hat{x}/\hat{a}$ and $y = \hat{y}/\hat{a}$ (where $\hat{x}$ and $\hat{y}$ are the corresponding real coordinates). The other dimensionless lengths shown in the Fig. 1b equals $a = \hat{a}/\hat{a} = 1$ and $0 < b = \hat{b}/\hat{a} \leqslant 1$. The relation between dimensionless and real stress

distributions is $\sigma(x,y)=\hat{\sigma}(x,y)\hat{a}^2/\hat{N}$ (where $\hat{\sigma}(x,y)$ and $\hat{N}$ are real normal stress and normal reaction, respectively).

The following relations between angles γ and γ' (defined in Fig. 1 and where $\boldsymbol{v}_r$ is velocity of deformation area F movement) hold

$$\cos\gamma'=\frac{\cos\gamma}{\sqrt{\cos^2\gamma+b^{-2}\sin^2\gamma}},\ \sin\gamma'=\frac{b^{-1}\sin\gamma}{\sqrt{\cos^2\gamma+b^{-2}\sin^2\gamma}}. \tag{6}$$

3.2. Integral model of dry friction

The relative motion of the body lying above the plane contact area F with respect the body lying below the region F, is the plane motion in the contact plane and can be described in a way shown in Fig. 1a, by the use of dimensionless velocity $\mathbf{v}_s=\hat{\mathbf{v}}_s/\hat{a}$ (of an arbitrarily chosen pole A) and angular velocity $\boldsymbol{\omega}_s$. Assuming the classical Coulomb friction law on each element dF of contact zone F, we can express it in the non-dimensional form $d\mathbf{T}_s=d\hat{\mathbf{T}}_s/(\mu\hat{N})=-\sigma(x,y)\mathbf{v}_P/\|\mathbf{v}_P\|dF$, where $d\mathbf{T}_s$ is infinitesimal dry friction force, $d\hat{\mathbf{T}}_s$ is its real counterpart, μ is dry friction coefficient, $\mathbf{v}_P=\hat{\mathbf{v}}_P/\hat{a}=\mathbf{v}_s+\boldsymbol{\omega}_s\times\boldsymbol{\rho}$ is non-dimensional velocity of the element dF (point P), where $\hat{\boldsymbol{v}}_P$ is real velocity of the point P and $\boldsymbol{\rho}=\hat{\boldsymbol{\rho}}/\hat{a}=\overrightarrow{AP}$ is dimensionless vector coupling the pole A with the element dF. Taking into account that infinitesimal dry friction torque is $d\mathbf{M}_s=d\hat{\mathbf{M}}_s/(\hat{a}\,\mu\hat{N})=\boldsymbol{\rho}\times d\mathbf{T}_s$, we get the following components of integral model of dry friction

$$T_{sx}(v_s,\omega_s,\varphi_s)=\iint_F\sigma(x,y)\frac{v_s\cos\varphi_s-\omega_s y}{m(v_s,\omega_s,\varphi_s)}dxdy,\ T_{sy}(v_s,\omega_s,\varphi_s)=\iint_F\sigma(x,y)\frac{v_s\sin\varphi_s+\omega_s x}{m(v_s,\omega_s,\varphi_s)}dxdy,$$

$$M_s(v_s,\omega_s,\varphi_s)=\iint_F\sigma(x,y)\frac{\omega_s(x^2+y^2)+v_s x\sin\varphi_s-v_s y\cos\phi_s}{m(v_s,\omega_s,\varphi_s)}dxdy, \tag{7}$$

where $m(v_s,\omega_s,\varphi_s)=\sqrt{(v_s\cos\varphi_s-\omega_s y)^2+(v_s\sin\varphi_s+\omega_s x)^2}$ and where the signs of the components has been changed. It means that the non-dimensional friction force and torque are $\mathbf{T}_s=-T_{sx}\mathbf{e}_x-T_{sy}\mathbf{e}_y$ and $\mathbf{M}_s=-M_s\mathbf{e}_z$ respectively (where $\mathbf{e}_x$, $\mathbf{e}_y$ and $\mathbf{e}_z$ are the unit vectors of the Cartesian coordinate system $Axyz$).

Exact integral forms Eq. (7) of the friction model are inconvenient for direct use in mathematical modelling and numerical simulations. The properties of integrals Eq. (7) with stress distribution given by Eq. (5), useful when constructing certain approximate models, are as follows

$$T_{sx}|_{v_s=0}=-c_{0,1,1}\delta_{\omega_s,1},\quad T_{sx}|_{\omega_s=0}=c_\varphi\delta_{v_s,1},\quad T_{sy}|_{v_s=0}=c_{1,0,1}\delta_{\omega_s,1},\quad T_{sy}|_{\omega_s=0}=s_\varphi\delta_{v_s,1},$$

$$M_s|_{v_s=0}=c_{0,0,-1}\delta_{\omega_s,1},\quad M_s|_{\omega_s=0}=(s_\varphi c_{1,0,0}-c_\varphi c_{0,1,0})\delta_{v_s,1},\quad \partial T_{sx}/\partial v_s|_{v_s=0}=c_\varphi c_{2,0,3}\delta_{\omega_s,0},$$

$$T_{sx}/\partial\omega_s|_{\omega_s=0}=-(s_\varphi^2 c_{0,1,0}+s_\varphi c_\varphi c_{1,0,0})\delta_{v_s,0},\quad \partial T_{sy}/\partial v_s|_{v_s=0}=s_\varphi c_{0,2,3}\delta_{\omega_s,0},$$

$$\partial T_{sy}/\partial\omega_s|_{\omega_s=0}=s_\varphi c_\varphi c_{1,0,0}\delta_{v_s,0},\quad \partial M_s/\partial v_s|_{v_s=0}=0,\quad \partial M_s/\partial\omega_s|_{\omega_s=0}=(s_\varphi^2(c_{0,2,0}-c_{2,0,0})+c_{2,0,0})\delta_{v_s,0},$$

$$\partial^2 T_{sx}/\partial\omega_s^2|_{\omega_s=0}=(3s_\varphi^2 c_\varphi(c_{2,0,0}-c_{0,2,0})-c_\varphi c_{2,0,0})\delta_{v_s,-1}, \tag{8}$$

$$\partial^2 T_{sy}/\partial\omega_s^2|_{\omega_s=0}=(3s_\varphi c_\varphi^2(c_{0,2,0}-c_{2,0,0})-s_\varphi c_{0,2,0})\delta_{v_s,-1},$$

$$\partial^2 M_s/\partial v_s^2|_{v_s=0}=(c_\varphi^2(c_{0,2,3}-c_{2,0,3})-c_{0,2,3})\delta_{\omega_s,-1},\quad \partial^2 M_s/\partial\omega_s^2|_{\omega_s=0}=3(s_\varphi c_\varphi^2(3c_{1,2,0}-c_{3,0,0})+$$

$$c_\varphi^3\left(3c_{2,1,0}-c_{0,3,0}\right)-s_\varphi c_{1,2,0}+c_\varphi\left(c_{0,3,0}-2c_{2,1,0}\right)\big)\delta_{v_s,-1},\quad \partial^3 T_{sx}/\partial\omega_s^3\big|_{\omega_s=0}=3\big(s_\varphi^4\left(5c_{0,3,0}-15c_{2,1,0}\right)+$$

$$+s_\varphi^3 c_\varphi\left(15c_{1,2,0}-5c_{3,0,0}\right)+s_\varphi^2\left(15c_{2,1,0}-4c_{0,3,0}\right)+s_\varphi c_\varphi\left(3c_{3,0,0}-6c_{1,2,0}\right)-2c_{2,1,0}\big)\delta_{v_s,-2},$$

$$\partial^3 T_{sy}/\partial\omega_s^3\big|_{v_s=0}=3\big(s_\varphi c_\varphi^3\left(5c_{0,3,0}-15c_{2,1,0}\right)+c_\varphi^4\left(15c_{1,2,0}-5c_{3,0,0}\right)+s_\varphi c_\varphi\left(6c_{2,1,0}-3c_{0,3,0}\right)+$$

$$+c_\varphi^2\left(4c_{3,0,0}-15c_{1,2,0}\right)+2c_{1,2,0}\big)\delta_{v_s,-2},$$

where the following notation has been used: $s_\varphi=\sin\varphi_s$, $c_\varphi=\cos\varphi_s$ and $\delta_{f,i}=f^i\,|f|^{-1}$ and where

$$c_{1,0,0}=\pi S_3 k_r\cos\gamma',\quad c_{0,1,0}=\pi b S_3 k_r\sin\gamma',\quad c_{0,1,1}=4bG(e)S_2 k_r\sin\gamma',\quad c_{1,0,1}=4H(e)S_2 k_r\cos\gamma',$$

$$c_{2,0,3}=4G(e)S_0,\quad c_{2,0,0}=\pi S_3,\quad c_{0,2,0}=\pi b^2 S_3,\quad c_{0,0,-1}=4E(e)S_2,\quad c_{0,2,3}=4H(e)S_0, \tag{9}$$

$$c_{1,2,0}=1/4\,\pi b^2 S_5 k_r\cos\gamma',\quad c_{2,1,0}=1/4\,\pi b S_5 k_r\sin\gamma',\quad c_{3,0,0}=3/4\,\pi\ S_5 k_r\cos\gamma',$$
$$c_{0,3,0}=3/4\,\pi b^3 S_5 k_r\sin\gamma',$$

while $K(e)$ and $E(e)$ are the complete elliptic integrals of the first and second kind, respectively, $G(e)=(K(e)-E(e))e^{-2}$, $H(e)=\big(E(e)+\left(e^2-1\right)K(e)\big)e^{-2}$, $S_i=\int_0^1 r'^i\,\sigma_0'(r')\,dr'$ and where $e=\sqrt{1-b^2}$ is eccentricity of the contact.

3.3. Hertz contact and piecewise polynomial approximation

For the approximation of the exact integral functions Eq. (7) we will use the following piecewise polynomial approximation ($v_s\geqslant 0$)

$$f^{(W_1)}(v_s,\omega_s,\varphi_s,\gamma',e)=\begin{cases}\operatorname{sgn}(\omega_s)\displaystyle\sum_{i=0}^{4}a_{f,i}(\varphi_s,\gamma',e)\left(\frac{v_s}{\omega_s}\right)^i & \text{for}\quad v_s\leqslant|\omega_s|u_{0,f}\\ \displaystyle\sum_{i=0}^{3}b_{f,i}(\varphi_s,\gamma',e)\left(\frac{\omega_s}{v_s}\right)^i & \text{for}\quad v_s>|\omega_s|u_{0,f},\end{cases} \tag{10}$$

where $f^{(W_1)}$ is the approximation of the function $f=T_{sx},T_{sy},M_s$.

Assuming that the approximating functions $T_{sx}^{(W_1)}$, $T_{sy}^{(W_1)}$ and $M_s^{(W_1)}$ satisfy all the derivatives Eq. (8) of exact integral model and that the pieces of the functions $f^{(W_1)}$ are joined in the points $v_s=|\omega_s|u_{0,f}$ ($u_{0,f}>0$) satisfying the continuity conditions of up to second order derivatives, one can easily find all the coefficients of the approximations Eq. (10) for the Hertz contact case ($\sigma_0'(r')=3/(2\pi)\sqrt{1-r'^2}$). The parameters $u_{0,T_{sx}}$, $u_{0,T_{sy}}$ and u_{0,M_s} defining the points of polynomial joining have been found as the following polynomials $u_{0,T_{sx}}(b)=0.967+0.276b-0.542b^2+0.706b^3$, $u_{0,T_{sy}}(b)=1.280+0.007b+0.106b^2$ and $u_{0,M_s}(b)=0.702+$ $+0.407b-0.819b^2+0.600b^3$ as a result of optimization of the fitting of the approximants to the exact integral model.

Assuming the Hertz theory, the parameter b is approximated as $b=\kappa^{-2/3}$ [8], where $\kappa=\kappa_2/\kappa_1$ is the ratio of relative principal curvatures κ_2 and κ_1, where $\kappa_2>\kappa_1$. Basing on the theory of surfaces of revolution [9] one can find that for the analysed celt (assuming $a_2=a_3$)

$$\kappa_1 = a_1 a_2 \left(a_1^2 - \left(a_1^2 - a_2^2 \right) a_1^{-2} r_{x_{1e}}^2 \right)^{-3/2}, \quad \kappa_2 = a_1 a_2^{-1} \left(a_1^2 - \left(a_1^2 - a_2^2 \right) a_1^{-2} r_{x_{1e}}^2 \right)^{-1/2}. \tag{11}$$

The size of the contact reads [8]

$$\hat{a} = \left(\frac{3\hat{N}}{4E^* \sqrt{\kappa_1 \kappa_2}} \right)^{1/3} F(e), \quad \text{where } F(e) = \left(\frac{4}{\pi e^2} \right)^{1/3} \left(\left(\frac{E(e)}{1-e^2} - K(e) \right) (K(e) - E(e)) \right)^{1/6} \tag{12}$$

where $E^* = \left((1-\nu_1^2)/E_1 + (1-\nu_2^2)/E_2 \right)^{-1}$ and where E_1, E_2, ν_1 and ν_2 are the Young's moduli and Poisson's ratios of the materials of two contacting bodies, respectively.

3.4. Other approximant models

Assuming no coupling between friction force and torque, one can propose the following model of friction

$$T_{sx}^{(O)} = \cos\varphi_s, \quad T_{sy}^{(O)} = \sin\varphi_s, \quad M_s^{(O)} = \operatorname{sgn}(\omega_s). \tag{13}$$

For more advanced modeling the following special forms of Padé approximations can be used ($v_s \geqslant 0$)

$$f^{(P_n')}(v_s, \omega_s, \varphi_s, \gamma', e) = \frac{\sum_{i=0}^{n} a_{f,i}(\varphi_s, \gamma', e, \operatorname{sgn}(\omega_s)) v_s^{n-i} \omega_s^i}{v_s^n + |\omega_s|^n}, \tag{14}$$

where one can find that

$$\partial^i f^{(P_n')} / \partial v_s^i \big|_{v_s=0} = i! a_{f,n-i} r, \qquad \partial^i f^{(P_n')} / \partial \omega_s^i \big|_{\omega_s=0} = i! a_{f,i} v_s^{-i} \tag{15}$$

where $r = \omega^{1-i}/|\omega|$ for n = 1,3,5,… and $r = \omega^{-i}$ for n = 2,4,6,… and where i = 0,1,2,…,n − 1.

Assuming n=1 and fulfilling the derivatives Eq. (8) of integral components up to zero order, we get

$$T_{sx}^{(P_1')} = \frac{v_{sx} - c_{0,1,1}\omega_s}{v_s + |\omega_s|}, \quad T_{sy}^{(P_1')} = \frac{v_{sy} + c_{1,0,1}\omega_s}{v_s + |\omega_s|}, \quad M_s^{(P_1')} = \frac{-c_{0,1,0}v_{sx} + c_{1,0,0}v_{sy} + c_{0,0,-1}\omega_s}{v_s + |\omega_s|}. \tag{16}$$

Assuming n = 3 and fulfilling the derivatives Eq. (8) of integral components up to first order, we get the following model

$$\begin{aligned}
T_{sx}^{(P_3')} &= \frac{v_s^2 v_{sx} - c_{1,0,0} v_{sx} v_{sy} \omega_s - c_{0,1,0} v_{sy}^2 \omega_s + c_{2,0,3} v_{sx} \omega_s^2 - c_{0,1,1} \omega_s^3}{v_s^3 + |\omega_s|^3}, \\
T_{sy}^{(P_3')} &= \frac{v_s^2 v_{sy} + c_{1,0,0} v_{sx}^2 \omega_s + c_{0,1,0} v_{sx} v_{sy} \omega_s + c_{0,2,3} v_{sy} \omega_s^2 + c_{1,0,1} \omega_s^3}{v_s^3 + |\omega_s|^3}, \\
M_s^{(P_3')} &= \frac{-c_{0,1,0} v_s^2 v_{sx} + c_{1,0,0} v_s^2 v_{sy} + c_{2,0,0} v_{sx}^2 \omega_s + c_{0,2,0} v_{sy}^2 \omega_s + c_{0,0,-1} \omega_s^3}{v_s^3 + |\omega_s|^3}.
\end{aligned} \tag{17}$$

Note that the friction model proposed in the work [5], when using our notation, takes the following form

$$T_{sx}^{(P_1)} = \frac{v_{sx}}{v_s + (8/3\pi)|\omega_s|}, \quad T_{sy}^{(P_1)} = \frac{v_{sy}}{v_s + (8/3\pi)|\omega_s|}, \quad M_s^{(P_1)} = 0. \tag{18}$$

3.5. Implementation of the friction and rolling resistance models to the celt model

The components of the friction and rolling resistance model occurring in the Eq. (1) read

$$\hat{\mathbf{T}}_s = -\mu\hat{N}\left(T_{sx}^{(a_\varepsilon)}\mathbf{e}_x + T_{sy}^{(a_\varepsilon)}\mathbf{e}_y\right),\ \hat{\mathbf{M}}_s = -\mu\hat{N}\,\hat{a}\,M_s^{(a_\varepsilon)}\mathbf{n},\ \hat{\mathbf{M}}_r = \hat{N}\,\hat{a}\,\pi\,S_3k_r\left(b\,s_{\gamma'}^{(\varepsilon)}\mathbf{e}_x - c_{\gamma'}^{(\varepsilon)}\mathbf{e}_y\right) \tag{19}$$

where the functions $T_{sx}^{(a_\varepsilon)}$, $T_{sy}^{(a_\varepsilon)}$ and $M_s^{(a_\varepsilon)}$ are the regularized versions of the components $T_{sx}^{(a)}$, $T_{sy}^{(a)}$ and $M_s^{(a)}$ (for a=W_1, O, P_1', P_3', P_1). The quantities where v_s, $\sin\varphi_s$, $\cos\varphi_s$, $\sin\gamma'$ and $\cos\gamma'$ are replaced by the functions $v_s^{(\varepsilon)}$, $s_\varphi^{(\varepsilon)}$, $c_\varphi^{(\varepsilon)}$, $s_{\gamma'}^{(\varepsilon)}$ and $c_{\gamma'}^{(\varepsilon)}$, defined in the following way

$$s_\varphi^{(\varepsilon)} = \frac{v_{sy}}{v_s^{(\varepsilon)}},\ c_\varphi^{(\varepsilon)} = \frac{v_{sx}}{v_s^{(\varepsilon)}},\ s_{\gamma'}^{(\varepsilon)} = \frac{v_{ry}'}{v_r'^{(\varepsilon)}},\ c_{\gamma'}^{(\varepsilon)} = \frac{v_{rx}'}{v_r'^{(\varepsilon)}}, \tag{20}$$

where $v_s^{(\varepsilon)} = \sqrt{v_{sx}^2 + v_{sy}^2 + \varepsilon}$, $v_r'^{(\varepsilon)} = \sqrt{v_{rx}^2 + b^{-2}v_{ry}^2 + \varepsilon}$, $v_{sx} = \mathbf{v}_s\cdot\mathbf{e}_x$, $v_{sy} = \mathbf{v}_s\cdot\mathbf{e}_y$, $v_{rx} = \mathbf{v}_r\cdot\mathbf{e}_x$ and $v_{ry} = \mathbf{v}_r\cdot\mathbf{e}_y$. Moreover, we assume that $M_s^{(O_\varepsilon)} = \omega_s\big/\sqrt{\omega_s^2+\varepsilon}$. The above regularization of the model with the small numerical parameter ε is performed in order to avoid set-valued friction laws and simplify the simulation process, and use classical integration methods of ordinary differential equations.

The non-dimensional sliding and rolling velocities and the spinning velocity are as follows

$$\mathbf{v}_s = \frac{\mathbf{v}_A}{\hat{a}},\ \mathbf{v}_r = \frac{d\mathbf{r}}{dt}\Big/\hat{a},\ \omega_s = \boldsymbol{\omega}\cdot\mathbf{n}, \tag{21}$$

where we have made an assumption, that the deformable Celtic stone rolls over a rigid table, since $d\mathbf{r}/dt$ is the relative velocity of the deformation zone in the material of the wobblestone. The same situation takes place under the assumption of non-slip rolling.

4. Numerical examples

In the numerical experiment we have assumed the mathematical model of the celt with the integral model of friction Eq. (7) and Hertz nominal stress distribution $\left(\sigma_0'(r') = 2/(3\pi)\sqrt{1-r'^2}\right)$, approximated by the model Eq. (10) (as a relatively good approximation) with corresponding regularizations ($W_{1\varepsilon}$) and with the following parameters: $m = 0.3$ kg, $g = 9.81$ m/s^2, $B_{x_{1e}} = 0.0003$ kg·m^2, $B_{x_{2e}} = 0.001$ kg·m^2, $B_{x_{3e}} = 0.001$ kg·m^2, $B_{x_{1e}x_{2e}} = 0.00023$ kg·m^2, $k_1 = k_2 = 0$, $k_3 = -0.005$ m, $a_1 = 0.11$ m, $a_2 = a_3 = 0.025$ m, $\mu = 0.25$, $k_r = 0.8$, $E^* = 10^8$ Pa. Then four approximate models (O_ε, $P_{1\varepsilon}'$, $P_{3\varepsilon}'$ and $P_{1\varepsilon}$) are optimized in order to fit one exemplary solution to model $W_{1\varepsilon}$ (see Fig. 3). In the regularized models we have assumed $\varepsilon = 10^{-5}$. In the process of optimization, the following parameters of the model have been obtained (we have assumed constant real characteristic dimension $\hat{a}$ of the contact patch): $\mu = 0.241$, $\hat{a} = 1.23$ mm, $b = 0.0060$, $S_3k_r = 0.595$ (model O_ε); $\mu = 0.262$, $\hat{a} = 1.06$ mm, $b = 0.0380$, $S_2 = 0.277$, $S_3 = 0.302$, $k_r = 0.414$ (model $P_{1\varepsilon}'$); $\mu = 0.250$, $\hat{a} = 2.30$ m, $b = 0.0994$, $S_0 = 0.095$, $S_2 = 0.121$, $S_3 = 0.111$, $k_r = 0.912$ (model $P_{3\varepsilon}'$); $\mu = 0.220$, $\hat{a} = 0.028$ mm (model $P_{1\varepsilon}$). In the case of simulation $P_{1\varepsilon}$, one have also assumed $S_3 = 0$, which implies no rolling resistance. Finally, the last model corresponds to that used in the work [5] (without friction torque and rolling resistance). The other parameters and initial conditions are the same as in the model $W_{1\varepsilon}$. The final values of the optimized function (being the average squared deviation between the corresponding components of the angular velocity of the celt) are: 0.067 rad^2 (O_ε), 0.042 rad^2 ($P_{1\varepsilon}'$), 0.007 rad^2 ($P_{3\varepsilon}'$) and 1.47 rad^2 (for $P_{1\varepsilon}$ model).

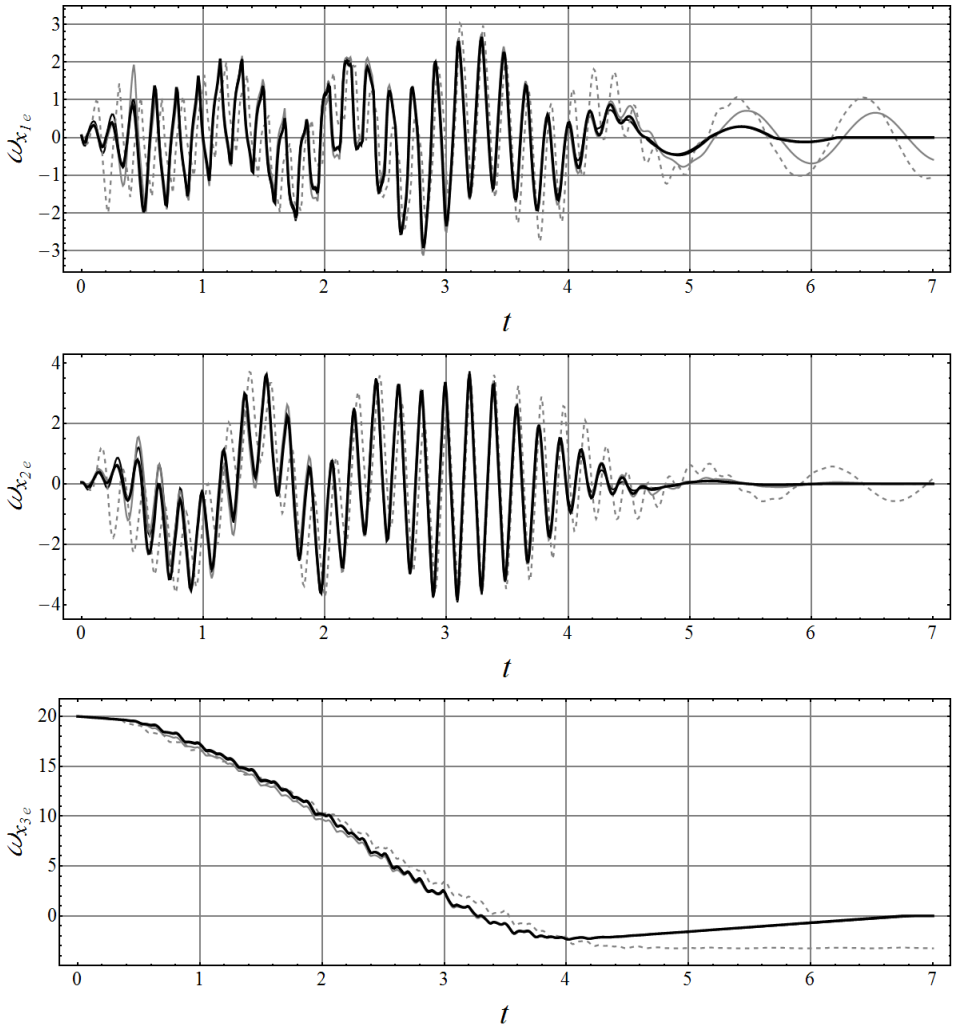

Fig. 3. The final fitting of the solutions to the models: $W_{1\varepsilon}$ (black thick line), O_ε (grey continuous line), $P_{1\varepsilon}$ (grey dashed line) and $P'_{3\varepsilon}$ (black thin line).

5. Concluding remarks

In the paper the approximate coupled models of friction and rolling resistance have been developed for the elliptic shape of the contact patch. In the presented numerical example it has been shown, that in the Celtic stone mathematical modeling and simulation, the coupling between friction force and torque can play certain role. However we expect that this effect will be more spectacular in certain other mechanical systems, where angular velocity of the contact patch is relatively large. Moreover the developed approximate models are ready to use in the case where the shape (eccentricity) of the contact is variable during the simulation process.

Acknowledgments

The work has been supported by the Ministry of Science and Higher Education under the grant no. 0040/B/T02/2010/38. J. Awrejcewicz acknowledges also a support of the Alexander von Humboldt Award.

References

[1] P. Contensou, *On Couplage entre frottement de glissement et de pivotement dans la t éorie de la toupe*, Kreiselprobleme Gyrodynamics: IUTAM Symp., Calerina, 1962, pp. 201−216.

[2] V.P. Zhuravlev, The model of dry friction in the problem of the rolling of rigid bodies, *Journal of Applied Mathematics and Mechanics* **62**(5) (1998), 705−710.

[3] V.P. Zhuravlev and A.A. Kireenkov, Pad éexpansions in the two-dimensional model of Coulomb frcition, *Mechanics of Solids* **40**(2) (2005), 1−10.

[4] A.A. Kireenkov, Combined model of sliding and rolling friction in dynamics of bodies on a rough surface, *Mechanics of Solids* **43**(3) (2008), 116−131.

[5] V.P. Zhuravlev and D.M. Klimov, Global motion of the celt, *Mechanics of Solids* **43**(3) (2008), 320−327.

[6] R.I. Leine and Ch. Glocker, A set-valued force law for spatial Coulomb-Contenou friction, *European Journal of Mechanics* **22**(2) (2003), 193−216.

[7] G. Kudra and J. Awrejcewicz, Tangens hyperbolicus approximations of the spatial model of friction coupled with rolling resistance, *International Journal of Bifurcation and Chaos* (2011), to appear.

[8] K.L. Johnson, *Contact Mechanics*, Cambridge University Press, Cambridge, 1985.

[9] A. Gray, *Surfaces of revolution*, Chapt. 20 in: Modern Differential Geometry of Curves and Surfaces with Mathematica, CRC Press, Boca Raton, 1997, pp. 457−480.